Comprehensive experimental and interpretational study of the complex formation and transformations involving o-quinoid molecules and an L3M-type metal fragment (M = cobalt)

ARTICLE *in* INORGANIC CHEMISTRY · NOVEMBER 1987

Impact Factor: 4.76 · DOI: 10.1021/ic00269a014

7 AUTHORS, INCLUDING:

Claudio Bianchini
Italian National Research Council
340 PUBLICATIONS **11,246** CITATIONS
SEE PROFILE

Carlo Mealli
Italian National Research Council
245 PUBLICATIONS **5,121** CITATIONS
SEE PROFILE

Andrea. Meli
Italian National Research Council
237 PUBLICATIONS **6,861** CITATIONS
SEE PROFILE

Piero Zanello
Università degli Studi di Siena
403 PUBLICATIONS **7,470** CITATIONS
SEE PROFILE

Reprinted from Inorganic Chemistry, 1987, 26, 3683

Contribution from the Istituto per lo Studio della Stereochimica ed Energetica dei Composti di Coordinazione, CNR, 50132 Firenze, Italy, Dipartimento di Chimica dell'Università di Firenze, 50100 Firenze, Italy, and Dipartimento di Chimica dell'Università di Siena, 53100 Siena, Italy

Comprehensive Experimental and Interpretational Study of the Complex Formation and Transformations Involving *o*-Quinoid Molecules and an L_3M-Type Metal Fragment (M = Cobalt)

Claudio Bianchini,*[1] Dante Masi,[1] Carlo Mealli,*[1] Andrea Meli,[1] Giacomo Martini,[2] Franco Laschi,[3] and Piero Zanello*[3]

Received April 10, 1987

Catecholate complexes of cobalt(II) and cobalt(III) with the tripodal phosphine $MeC(CH_2PPh_2)_3$ (triphos) have been synthesized either by oxidative addition of *o*-benzoquinones to (triphos)Co fragments or by chloride ligand replacement by catecholates on $[(triphos)Co(\mu\text{-}Cl)_2Co(triphos)]^{2+}$ (*o*-benzoquinone = 3,5-di-*tert*-butyl-*o*-benzoquinone (3,5-DBQ), tetrachloro-*o*-benzoquinone (*o*-Cl_4Q), 9,10-phenanthrenequinone (phenQ); catecholate = 3,5-DBCat, *o*-Cl_4Cat, phenCat). These complexes undergo electron-transfer reactions that encompass the Co(III), Co(II), and Co(I) oxidation states of the metal and the catecholate, semiquinone, and quinone oxidation levels of the quinoid ligand. Electrochemical techniques have been used to prepare some species not directly obtainable by chemical methods such as the semiquinone derivatives. The characterization has been carried out by IR, ^1H and ^{31}P NMR, and EPR techniques. The structure of $[(triphos)Co(3,5\text{-}DBCat)]BPh_4 \cdot 0.5\ C_4H_9OH \cdot C_2H_5OH$ (**2**) has been established by an X-ray analysis. Crystal data: monoclinic, space group $P2_1/a$ with a = 45.940 (8) Å, b = 19.945 (5) Å, c = 16.093 (4) Å, β = 98.94 (3)°, Z = 8, R = 0.078 (R_w = 0.087) for 5028 unique reflections. The two independent $[(triphos)Co(3,5\text{-}DBCat)]^+$ cations in the asymmetric unit of the crystal of **2** are geometrically very similar. The triphos and the 3,5-DBCat ligands determine a distorted-square-pyramidal geometry about the cobalt atom. A MO qualitative analysis describes the relevant features of the members of the series of electronic isomers. A reasonable hypothesis is forwarded for the mechanism of electron transfer from the metal to the ligand in the genesis of the very stable Co(III) catecholate complexes. Finally, it is shown that the redox properties, not experimentally shown by analogous tropolonate compounds, are due to the unique electronic nature of the six-membered C_6 ring substituted in ortho positions by two chalcogen atoms.

Introduction

Multielectron sequential redox changes are characteristic of complexes formed by transition-metal fragments with members of the family of *o*-quinoid molecules, which include benzoquinones, (I), semiquinones (II), and catecholates (III).[4] Also, the compounds in question are generally considered valid models for several biological processes involving electron transfers such as bacterial photosynthesis.[5] In addition, metal–catecholate interactions are well recognized to occur in microbial iron transport reagents and dioxygenase enzymes.[6]

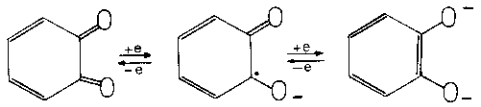

I II III

Much effort has been devoted to the understanding of the subtle link that relates the oxidation state of the metal and the nature of the ligand[4], including theoretical studies.[7] The stepwise reduction of the *o*-benzoquinone ligand occurs usually at the expense of metal electrons. The process is often referred to as oxidative addition. A schematic representation of this type of oxidative process is depicted in IV. A σ bond is broken within the X–Y ligand. In MO terms a two-way flow of electron density from X–Y to the metal and in the reverse direction accounts for the formation of new M–X and M–Y bonds.

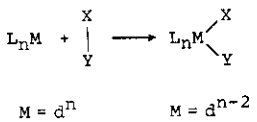

$M = d^n$ $M = d^{n-2}$

IV

As shown in V, two electrons, initially populating a metal π hybrid, are transferred into a σ^* MO of the ligand, thus causing the X–Y cleavage. In the formation of catecholate complexes from *o*-benzoquinones, is the metal to ligand electron transfer governed by a similar mechanism? Why do 1,2-diones supported by a seven-membered C_7 ring (tropolonate), VI, not have the same *noninnocent* character of the quinoid species?

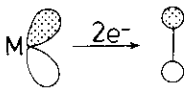

V

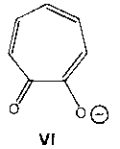

VI

In order to shed some light on the points, we have investigated a number of reactivity patterns between metal fragments $[(triphos)Co]^n$ [triphos = $MeC(CH_2PPh_2)_3$; n = 0, 2+] and some *o*-quinoid compounds of type I or III. The nature of the reactants was changed as systematically as possible by varying the metal oxidation state in the fragment (triphos)Co and alternating the type of ligand I or III. Electrochemical and EPR techniques were used to isolate and characterize important intermediates not directly obtainable by chemical methods. Parallel attempts were made to develop a similar chemistry of the tropolonate ligand. The results are critically evaluated with the help of qualitative MO arguments based on extended Hückel calculations.

Results and Discussion

Synthesis and Characterization of the Compounds. Blue crystals of the catecholate complex $[(triphos)Co(3,5\text{-}DBCat)]ClO_4$ (**1**) are obtained by adding a CH_2Cl_2 solution of 3,5-di-*tert*-butyl-*o*-benzoquinone (3,5-DBQ) to an equimolecular mixture of $Co(ClO_4)_2$ and triphos in CH_2Cl_2/ethanol (eq 1).

$$Co(ClO_4)_2 + triphos + 3,5\text{-}DBQ \xrightarrow{CH_2Cl_2/EtOH} [(triphos)Co(3,5\text{-}DBCat)]ClO_4 \quad (1)$$

(1) CNR.
(2) Dipartimento di Chimica dell'Università di Firenze.
(3) Dipartimento di Chimica dell'Università di Siena.
(4) For a review on the metal chemistry of *o*-quinoid molecules see: (a) Pierpont, C. G.; Buchanan, R. M. *Coord. Chem. Rev.* **1981**, *38*, 45. For more recent or significative articles see: (b) Larsen, S. K.; Pierpont, C. G.; DeMunno, G.; Dolcetti, G. *Ibid.* **1986**, *25*, 4828. (c) Cass, M. E.; Gordon, N. R.; Pierpont, C. G. *Ibid.* **1986**, *25*, 3962. (d) Buchanan, R. M.; Pierpont, C. G. *Ibid.* **1980**, *102*, 4951.
(5) Wraight, C. A. *Photochem. Photobiol.* **1979**, *30*, 767.
(6) (a) Raymond, K. N.; Carrano, C. J. *Acc. Chem. Res.* **1979**, *12*, 183. (b) Que, L., Jr. *Struct. Bonding (Berlin)* **1980**, *40*, 39.
(7) (a) Gordon, D. J.; Fenske, R. F. *Inorg. Chem.* **1982**, *21*, 2907. (b) *Ibid.* **1982**, *21*, 2916.

Table I. Bond Lengths (Å) and Angles (deg) for [(triphos)Co(3,5-DBCat)]BPh_4·0.5C_4H_9OH·C_2H_5OH

	molecule a	molecule b		molecule a	molecule b		molecule a	molecule b
Co_1–P_1	2.222 (6)	2.206 (5)	C_{15}–C_{16}	1.382 (28)	1.368 (22)	P_1–Co_1–P_2	92.5 (5)	94.8 (2)
Co_1–P_2	2.200 (5)	2.194 (6)	C_{16}–C_{11}	1.452 (25)	1.435 (22)	P_1–Co_1–P_3	89.8 (2)	90.4 (2)
Co_1–P_3	2.207 (5)	2.193 (5)	C_{14}–C_{17}	1.582 (29)	1.545 (24)	P_2–Co_1–P_3	90.3 (2)	88.9 (2)
Co_1–O_1	1.880 (1)	1.887 (10)	C_{16}–C_{18}	1.507 (27)	1.537 (25)	P_1–Co_1–O_1	93.2 (4)	90.8 (3)
Co_1–O_2	1.851 (12)	1.836 (11)	P_1–C_1	1.840 (16)	1.867 (17)	P_1–Co_1–O_2	161.3 (4)	156.7 (4)
O_1–C_{11}	1.337 (22)	1.323 (17)	P_2–C_2	1.832 (18)	1.865 (16)	P_2–Co_1–O_1	111.3 (4)	112.2 (4)
O_2–C_{12}	1.358 (21)	1.343 (19)	P_3–C_3	1.823 (18)	1.857 (15)	P_2–Co_1–O_2	105.7 (4)	108.2 (4)
C_{11}–C_{12}	1.398 (26)	1.375 (22)	C_1–C_4	1.511 (24)	1.516 (24)	P_3–Co_1–O_1	158.1 (4)	158.7 (4)
C_{12}–C_{13}	1.430 (28)	1.431 (22)	C_2–C_4	1.613 (26)	1.576 (24)	P_3–Co_1–O_2	85.8 (4)	86.6 (4)
C_{13}–C_{14}	1.391 (25)	1.389 (25)	C_3–C_4	1.634 (24)	1.540 (23)	O_1–C_{11}–C_{12}	114.6 (1.6)	113.8 (1.4)
C_{14}–C_{15}	1.445 (27)	1.428 (24)	C_5–C_4	1.514 (23)	1.515 (23)	O_2–C_{12}–C_{11}	113.8 (1.6)	115.5 (1.4)

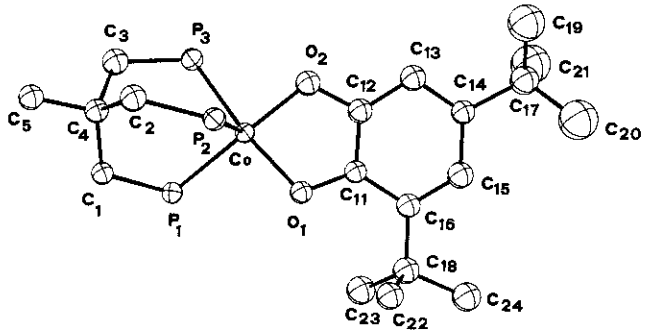

Figure 1. View, perpendicular to the plane of the catecholate ligand, of one of the two independent complex [(triphos)Co(3,5-DBCat)]$^+$ cations (cation a) present in the asymmetric unit of the monoclinic cell.

Compound **1** is diamagnetic and air-stable both in the solid state and in solution. It is soluble in common organic solvents in which it behaves as a 1:1 electrolyte (molar conductance in 10^{-3} M nitroethane solution: 45 Ω^{-1} cm^2 mol^{-1}). The $^{31}P\{^1H\}$ NMR spectrum ($CDCl_3$, 293 K) consists of a singlet at 31.88 ppm. Such a pattern does not vary over the temperature range 308–213 K and is consistent with the rapid intramolecular exchange of the three phosphorus atoms of triphos around the cobalt atom as commonly found in five-coordinate triphos complexes.[8] The ^1H NMR spectrum ($CDCl_3$, 293 K) exhibits *tert*-butyl resonances at 1.42 and 1.37 ppm. The IR spectrum shows no ν(C=O), whereas absorption bands at 1230 and 1210 cm^{-1} are observed that may be attributed to ν(C—O) of a coordinated catecholate.[9]

Metathetical reaction of **1** in CH_2Cl_2 with $NaBPh_4$ in 1-butanol/ethanol affords [(triphos)Co(3,5-DBCat)]BPh_4·0.5C_4H_9OH·C_2H_5OH (**2**) as well-formed blue crystals that were studied through X-ray methods.

There are two independent couples of [(triphos)Co($O_2C_{14}H_{20}$)]$^+$ cations and BPh_4 anions in the asymmetric unit of the crystal of **2**.

Table I reports a comparative selection of bond distances and angles relative to the two complex cations one of which, cation a, is shown in Figure 1. The geometrical differences between the two cations are only marginal. In cation b the two *tert*-butyl groups are equally oriented in the sense that one of the terminal carbon atoms lies almost in the plane of the six-membered ring (for both groups one torsion angle at the exocyclic C–C bond is close to 0°, e.g. −3.7 and −11.3° for the torsion angles C_{13}–C_{14}–C_{17}–C_{20} and C_{15}–C_{16}–C_{18}–C_{22}, respectively). For cation a the *tert*-butyl group linked to the atom C_{16} maintains the same orientation as the groups in cation b (smallest torsion angle −12.0°) whereas no terminal C–C bond of the *tert*-butyl group linked to C_{14} is coplanar with the aromatic ring (smallest torsion angle −26.4°). Although this feature can justify the packing of the pairs of cations and anions in the asymmetric unit, the environment about each metal is practically the same so that in our discussion we can refer to an average five-coordinate complex.

The P_3Co grouping of the (triphos)Co fragment has an approximate C_{3v} symmetry with three P–Co–P angles in the range 88.9–94.9°. The bidentate catecholate ligand is oriented in such a way that no Co–P bond lies in the plane of the catecholate. If so, the geometry would approximate a trigonal bipyramid with one equatorial and one axial oxygen donor. In actuality, the coordination approximates better a square pyramid. This square-pyramid-like geometry was already found in other (triphos)(O-O)Co(II) complexes where O-O is a chelate with two oxygen donors such as acetate,[10] sulfate,[11] or selenate.[10] Although on the NMR scale the equivalence of the three phosphorus atoms suggests rapid interconversion between the trigonal bipyramid and the square pyramid, the solid-state structure indicates an energetic preference for the latter geometry.

Of particular interest for our purposes is the bonding within the metallocycle Co–O–C–C–O and within the C_6 ring. A direct comparison can be made with the closely related cobalt complex [η^5-$C_5(CH_3)_5$]Co($O_2C_6H_4$)[12] where a [η^5-$C_5(CH_3)_5$]Co unit is in place of the isolobal (triphos)Co$^+$ fragment. Concerning the metallocycle, the average C–O and C–C distances of 1.346 (8) and 1.385 (5) (average) in **2** compare relatively well with the values 1.338 (3) and 1.408 (4) Å in the above-mentioned compound. Also the Co–O distances are very similar in the two compounds, being 1.863 (16) and 1.837 (2) Å, respectively. Unfortunately, the standard deviations in **2** are about five times larger than those affecting the cyclopentadienylcobalt complex, and a detailed discussion may sound specious. Thus it suffices to point out that the C–C bonds adjacent to the metallocycle C–C bond (C_{12}–C_{13} and C_{11}–C_{16}) as well as that trans to it (C_{14}–C_{15}) are significantly elongated [1.44 (1) (average) Å] with respect to the 1.39 Å value of benzene. Also, the Co–O distances in **2** are significantly shorter than those found in other complexes containing the (triphos)Co fragment coordinated by a O-O chelate, e.g. the cation [(triphos)Co(acetate)]$^+$ in which the Co–O bonds average 2.014 (19) Å.[10] The shortening in **2** can be attributed to a sort of π conjugation within the five-membered metallocycle as will become clear in the light of the subsequent MO considerations. As an anticipation, for the metal electron count (d^7) in [(triphos)Co(acetate)]$^+$, one electron not available in **2** in located in a $\pi_\perp$* antibonding orbital between the metal and the pair of oxygen atoms. As a consequence both Co–O distances are expected to be elongated.

Given the catecholate nature of the ligand and the diamagnetism of **2**, the metal can be assumed to be Co(III) and the complex a formal d^{16}-electron species. If we recall that the initial reagents were *o*-benzoquinone and a cobalt(II) salt, we are forced to conclude that one electron was extracted from the external environment to form the final complex. In order to understand better this fact we have attempted to obtain **1** or **2** from other reagents carrying different electron counts on the side either of the metal or of the ligand.

Reaction of preformed 3,5-di-*tert*-butylcatecholate anions in ethanol with a CH_2Cl_2 solution of the Co(II) dimer [(triphos)-

(8) Bianchini, C.; Meli, A.; Scapacci, G. *Organometallics* **1985**, *4*, 264.
(9) Sofen, S. R.; Ware, D. C.; Cooper, S. R.; Raymond, K. N. *Inorg. chem.* **1979**, *18*, 234.
(10) Mealli, C.; Midollini, S.; Sacconi, L. *Inorg. Chem.* **1975**, *14*, 2513.
(11) Benelli, C.; DiVaira, M.; Noccioli, G.; Sacconi, L. *Inorg. Chem.* **1977**, *16*, 182.
(12) Miller, E. J.; Rheingold, A. J.; Brill, T. B. *J. Organomet. Chem.* **1984**, *273*, 377.

$Co(\mu\text{-}Cl)_2Co(triphos)](ClO_4)_2$[13] yields **1** (eq 2). The latter compound can be obtained also by adding $(NBu_4)ClO_4$ in ethanol to an equivalent mixture of triphos, $Co_2(CO)_8$, and 3,5-DBQ (eq 3).

$$0.5[(triphos)Co(\mu\text{-}Cl)_2Co(triphos)](ClO_4)_2 + 3,5\text{-DBCat} \xrightarrow{CH_2Cl_2/EtOH} [(triphos)Co(3,5\text{-DBCat})]ClO_4 \quad (2)$$

$$0.5Co_2(CO)_8 + triphos + 3,5\text{-DBQ} \xrightarrow{THF/EtOH} [(triphos)Co(3,5\text{-DBCat})]^+ \quad (3)$$

The 1:2 reaction of $Co_2(CO)_8$ and triphos is known to provide a plain method to generate in solution (triphos)Co(0)(d^9) fragments that may be stabilized by appropriate coligands.[14] In the presence of 3,5-DBQ an instant reaction occurs as shown by the violet color assumed by the solution. On addition of *n*-pentane, a brown violet powder is precipitated (eq 4). All our attempts

$$0.5Co_2(CO)_8 + triphos + 3,5\text{-DBQ} \xrightarrow{THF/n\text{-pentane}} (triphos)Co(3,5\text{-DBCat}) \quad (4)$$

to recrystallize this product met without success because of its instability in solution, particularly as related to oxygen and protic solvents. As a matter of fact, although handled with extreme care, violet THF or MeCN solutions turn blue within some minutes. In particular, we note that the addition of ethanol causes an immediate color change (see reactions 2 and 3). On subsequent addition of $(NBu_4)ClO_4$ or $NaBPh_4$ crystals of **1** and **2** are formed, respectively. The reflectance spectrum of the brown violet product of reaction 4, with absorption maxima at 12390, 16316 and 20050 cm^{-1}, is typical of low-spin five-coordinate Co(II) complexes of triphos.[13] The compound is paramagnetic with a room-temperature magnetic moment corresponding to one unpaired spin (μ_{eff} = 2.08 μ_B). It is therefore reasonable to conclude that the violet compound is the neutral cathecolate complex (triphos)Co(3,5-DBCat) (**3**). In nice agreement with this formulation, **3** can be obtained by reduction of the cobalt(III) catecholate with $Co(Cp)_2$ (eq 5).

$$[(triphos)Co(3,5\text{-DBCat})]^+ + Co(Cp)_2 \rightarrow (triphos)Co(3,5\text{-DBCat}) + [Co(Cp)_2]^+ \quad (5)$$

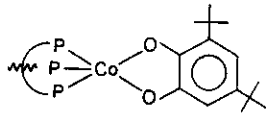

3

A fast interconversion between square-pyramidal and trigonal-bipyraidal geometries characterizes the solution behavior of the Co(III) derivative **2**. In actuality, there is no reason to believe that an extra electron in the system may raise a high energy barrier for such an interconversion. As a matter of fact, it is reasonable to assume that an almost equivalent mixture of square-pyramidal and trigonal-bipyramidal species is present in ambient temperature solutions of **3**, as indicated by the EPR spectrum in MeCN (Figure 2a) or CH_2Cl_2 at 290 K. This clearly shows that two complex species A and B are present with $\langle g_A \rangle$ = 2.145 ($\langle A_{Co} \rangle$ = 40 × 10^{-4} cm^{-1}) and $\langle g_B \rangle$ = 2.053 ($\langle A_{Co} \rangle$ = 39 × 10^{-4} cm^{-1}).

Interestingly, the EPR spectra in MeCN or CH_2Cl_2 glasses at 100 K show the existence of one species only. The spectrum in MeCN, which is shown in Figure 2b, can be interpreted by using a $S = {}^1/_2$ spin Hamiltonian with g_1 = 2.19 (A_1 = 68 × 10^{-4} cm^{-1}), $g_2 \simeq 2.07$ (A_2 = 58 × 10^{-4} cm^{-1}), and g_3 = 1.98 (A_3 = 50 × 10^{-4} cm^{-1}), the hyperfine coupling being with the ^{59}Co nucleus ($I = {}^7/_2$). The Hamiltonian parameters are consistent either with square-planar or square-pyramidal geometries around low-spin

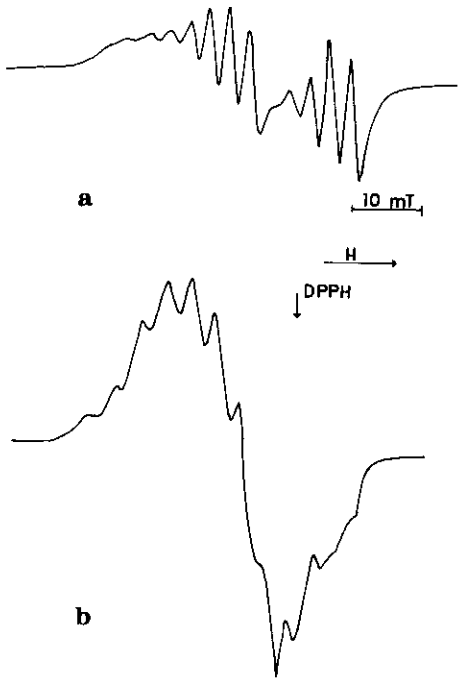

Figure 2. (a) X-Band EPR spectrum of **3** in MeCN solution at 290 K. (b) Spectrum in MeCN frozen solution at 100 K.

Co(II) ions.[15] In the latter case, however, a weak cobalt–phosphorus (apical) interaction should take place. The powder EPR spectrum (298 K) does not discriminate between any possible geometry in the solid state as it consists of a single broad resonance at $\langle g \rangle$ = 2.089, indicative of strong exchange interactions between nearest neighbors.

Reaction 4 is not very surprising. Cobalt(0), a d^9 species, carries a sufficient number of electrons to reduce the *o*-quinone to catecholate while maintaining one unpaired electron. The difficulty in isolating the paramagnetic cobalt(II) product is a clear indication that the unpaired electron is labile and that the cobalt(III) compound **2** is definitely more stable (see reactions 1–3). Additional experimental support to the proposed formulation of **3** is provided by the electrochemical studies reported in the following section as well as by the reactions of other *o*-benzoquinones such as 9,10-phenanthrenequinone (phenQ) and tetrachloro-1,2-benzoquinone (*o*-Cl_4Q) with (triphos)Co fragments.

Identical reactivity toward both (triphos)Co(II) and (triphos)Co(0) is displayed by 9,10-phenanthrenequinone, phenQ, and by tetrachloro-*o*-benzoquinone, *o*-Cl_4Q. The monocationic cobalt(III) catecholate derivatives $[(triphos)Co(phenCat)]^+$ and $[(triphos)Co(o\text{-}Cl_4Cat)]^+$ can be isolated as ClO_4^- or BPh_4^- salts. The Co(II) complex (triphos)Co(*o*-Cl_4Cat) (**4**), which appears as the most stable member of the present Co(II) series, can be prepared by three different synthetic routes including electrolysis at controlled potential of the Co(III)–*o*-Cl_4Cat derivative (see the following section). The chemical routes are shown in (6) and (7).

$$Co_2(CO)_8 + 2\ triphos + 2o\text{-}Cl_4Q \xrightarrow{THF/n\text{-pentane}} 2(triphos)Co(o\text{-}Cl_4Cat) + 8CO \quad (6)$$

$$[(triphos)Co(o\text{-}Cl_4Cat)]^+ + Co(Cp)_2 \xrightarrow{MeCN} (triphos)Co(o\text{-}Cl_4Cat) + [Co(Cp)_2]^+ \quad (7)$$

Compound **4** can be isolated as nice, orange brown crystals by route 7. The compound is nonconducting in nitroethane and paramagnetic (μ_{eff} = 2.02 μ_B at 298 K). The UV–visible spectrum with absorption maxima at 11299, 16666, and 21050 cm^{-1} is fully comparable with those of five-coordinate low-spin Co(II) com-

(13) Sacconi, L.; Mani, F. *Transition Met. Chem. (N.Y.)* **1982**, *8*, 179.
(14) Bianchini, C.; Mealli, C.; Meli, A.; Orlandini, A.; Sacconi, L. *Inorg. Chem.* **1980**, *19*, 2968.
(15) Bencini, A.; Gatteschi, D. *Transition Met. Chem. (N.Y.)* **1982**, *8*, 1.

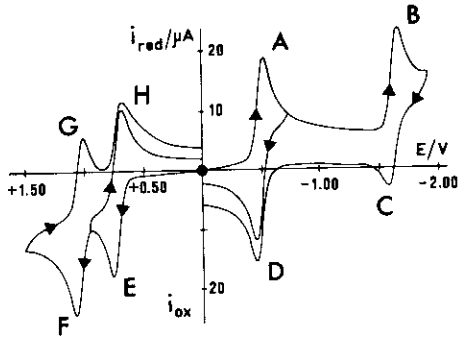

Figure 3. Cyclic voltammetric response recorded at a platinum electrode on a MeCN solution containing **1** (1.1×10^{-3} mol dm^{-3}) and $[NEt_4]ClO_4$ (0.1 mol dm^{-3}). Scan rate: 0.2 V s^{-1}. ● indicates starting potential.

plexes with triphos.[13] On the basis of all of these data, **4** is assigned the following structure:

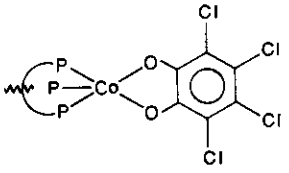

4

The EPR behavior of **4** (powder, solution, and frozen solution) is essentially identical with that of **3**, thus confirming that the two compounds share magnetic and structural features (EPR data are reported in the Experimental Section).

Our next step was that of exploring the behavior of other bidentate ligands able to form Co–O–C–C–O metallorings. In particular, our attention was focused on the tropolonato ion (VI). No electron-transfer chemistry was expected for the complexes of this anion, but we wished to understand the intrinsic reasons for the different behavior.

Tropolone (2-hydroxy-2,4,6-cycloheptatrien-1-one) reacts with a mixture of $Co(ClO_4)_2$ and triphos in CH_2Cl_2/EtOH to give air-stable green crystals of $[(triphos)Co(O_2C_7H_5)]ClO_4$ (**5**). An excess of triphos is necessary to have a good yield (85%). In fact, the triphos ligand besides functioning as coligand, deprotonates tropolone to the tropolonato ion (eq 8).[10]

$$2triphos + Co^{2+} + HO_2C_7H_5 \rightarrow [(triphos)Co(O_2C_7H_5)]^+ + triphosH^+ \quad (8)$$

Compound **5** is paramagnetic with a magnetic moment corresponding to one unpaired spin (μ_{eff} = 2.08 μ_B, 298 K). It is soluble in common organic solvents in which it behaves as a 1:1 electrolyte (molar conductance value in 10^{-3} M nitroethane solution: 47 Ω^{-1} cm^2 mol^{-1}). The reflectance spectrum with absorption maxima at 10869, 14814, and 23529 cm^{-1} is very similar to those of five-coordinate low-spin d^7 complexes that have been mentioned to have an approximate square-pyramidal geometry such as $(triphos)Co(SO_4)$, $[(triphos)Co(acetate)]BPh_4$, and $[(triphos)Co(acac)]BPh_4$.[13] Accordingly, also **5** is assigned this type of structure, which ultimately is very similar to that of **2** (Figure 1). EPR data for **5** are reported in the Experimental Section and are fully comparable with those of **3** and **4**.

The formation of a stable cobalt(II) tropolonate is also consistent with the absence of a proper redox activity of the tropolonato ion, and this indirectly emphasizes the unique role of the quinoid ligands in determining the formal oxidation state of the complexed metals. A rationale for this fact is presented in the following MO section. Before that the results of our electrochemical studies must be illustrated.

Electrochemistry. Figure 3 shows the cyclic voltammetric behavior of **1** at a platinum electrode in deaereated MeCN solution. Two subsequent cathodic processes (at peaks A and B, respectively) and two subsequent anodic processes (at peaks E and F, respectively) are displayed.

Controlled-potential coulometric experiments performed at the potential of the first reduction process (at −0.9 V) are consistent with the consumption of 1 mol of electrons/mol of **1**. Cyclic voltammetry at scan rates, v, ranging from 0.02 to 50 V s^{-1} shows for this cathodic step the typical features of an uncomplicated reversible one-electron charge transfer (i_{pD}/i_{pA} = 1; $i_{pA}/v^{1/2}$ = constant; $E_{pD} - E_{pA} = \Delta E_p \simeq 60$ mV).[16] The first reduction process can be attributed to the metal-centered charge-transfer (9).

$$[(triphos)Co(3,5\text{-}DBCat)]^+ \underset{-e^-}{\overset{+e^-}{\rightleftharpoons}} (triphos)Co(3,5\text{-}DBCat) \quad (9)$$
$$E^{\circ\prime} = -0.49 \text{ V}$$

After the exhaustive one-electron cathodic reduction at a platinum macroelectrode, the cyclic voltammetric response relevant to the peak system A/D, now reversed, exhibits the same diagnostic features. This suggests that no major change occurs in the skeleton of **1** as a consequence of the Co(III)/Co(II) redox change. Interestingly, during the redox step (eq 9) the color of the solution changes from blue to violet and vice versa. The reflectance and EPR spectra of the violet solid obtained by solvent elimination under reduced pressure are identical with those of the product of the reaction of (triphos)Co(0) with 3,5-DBQ, thereby confirming that the *o*-quinone extracts two electrons from the metal. The peak height of the cathodic process occurring at the potentials of the peak system B/C is consistent with a one-electron Co(II)/Co(I) charge transfer. The analysis of the relevant cyclic voltammograms with scan rates reveals the following features: $i_{pC}/i_{pB} < 1$ for scan rates lower than 5 V s^{-1}; $i_{pB}/v^{1/2}$ slightly decreases with scan rate; $E_{pC} - E_{pB} = \Delta E_p$ gradually increases from 90 mV at 0.02 V s^{-1} to 200 mV at 20 V s^{-1}. These data indicate that a homogeneous chemical reaction follows the one-electron quasi-reversible Co(II)/Co(I) charge transfer. If a first order chemical reaction corresponds to the decomposition of the electrogenerated cobalt(I) catecholate complex, a half-life time of about 2–3 s can be grossly computed.[17] In conclusion, the electrode mechanism for the second cathodic step can be schematized as (10).

$$(triphos)Co(3,5\text{-}DBCat) \underset{-e^-}{\overset{+e^-}{\rightleftharpoons}} [(triphos)Co(3,5\text{-}DBCat)]^- \xrightarrow[t_{1/2} = 2\text{–}3 \text{ s}]{E^\circ = -1.63 \text{ V}} \text{decomposition products} \quad (10)$$

In accordance with the electrochemical behavior of some molybdenum(VI),[18] ruthenium(II),[19] and cobalt(III)[20] catecholate complexes, the two anodic steps occurring at the peak systems E/H and F/G are assigned to the well-known ligand-centered one-electron sequential processes I–III.

The analysis of the relevant cyclic voltammograms with scan rates shows that both of the charge transfers Cat/SQ and SQ/Q are almost reversible in character but complicated by subsequent chemical reactions. Controlled-potential coulometric experiments performed in correspondence to the first anodic step at +0.78 V show that after the consumption of 1e/molecule, the current significantly decreases but remains higher than the background current up to the overall consumption of 2 mol of electrons/mol of **1**. During this process the blue starting solution turns green and then slowly assumes a yellow-brown color. The same result is also obtained when the macroelectrolysis is performed at the potential of the second anodic step at +1.3 V. The cyclic voltammogram recorded on the solution after the exhaustive two-electron anodic oxidation displays the following picture: two close

(16) Brown, E. R.; Large, R. F. *Physical Methods of Chemistry*; Weissberger, A. Rossiter, B. W., Eds.; Wiley-Interscience: New York, 1971; Vol. 1, p 423.
(17) Nicholson, R. S.; Shain, I. *Anal. Chem.* **1964**, *36*, 706.
(18) Bradbury, J. R.; Schultz, F. A. *Inorg. Chem.* **1986**, *25*, 4416.
(19) (a) Balch, A. L. *J. Am. Chem. Soc.* **1973**, *95*, 2723. (b) Girgis, A. Y.; Sohn, Y. S.; Balch, A. L. *Inorg. Chem.* **1975**, *14*, 2327. (c) Connelly, N. G.; Manners, I.; Protherol, J. R. C.; Whiteley, M. W. *J. Chem. Soc., Dalton Trans.* **1984**, 2713. (d) Haga, M.; Dodsworth, E. S.; Lever, A. B. P. *Inorg. Chem.* **1986**, *25*, 447.
(20) Wicklund, P. A.; Brown, D. G. *Inorg. Chem.* **1976**, *15*, 396.

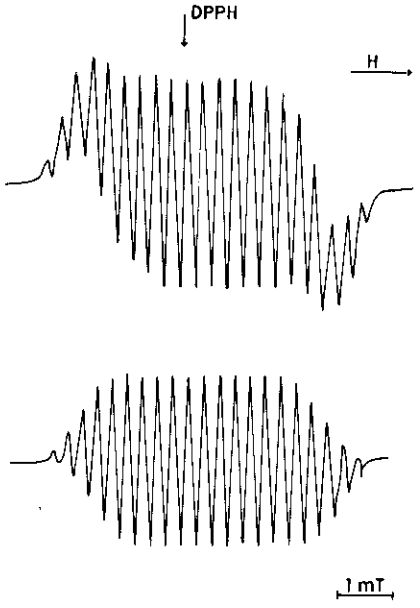

Figure 4. Experimental (upper) and computed (lower) X-band EPR spectra of electrogenerated [(triphos)Co(3,5-DBSQ)]$^{2+}$ in MeCN–$[NEt_4]ClO_4$ (0.1 mol dm^{-3}) at 290 K.

cathoanodic peak systems located at the formal potentials of −0.52 and −0.40 V, respectively; a cathodic peak at +0.44 V to which no reoxidation peak can be directly associated.

The electrolysis product obtained at the first anodic process after the consumption of 1e/molecule was examined by EPR spectroscopy. The EPR data (MeCN solution, temperature range 230–305 K) are in nice agreement with the electrochemical results.

Figure 4 shows the experimental and calculated spectra. The following coupling constants have been used to compute the spectrum: $\langle A_{Co}\rangle = 5.4 \times 10^{-4}$ cm^{-1}, $\langle A_P\rangle = 5.4 \times 10^{-4}$ cm^{-1} for one ^{31}P nucleus and 2.7×10^{-4} cm^{-1} for the other two ^{31}P nuclei, and, finally, 2.7×10^{-4} cm^{-1} for the two ring protons. The average $\langle g\rangle$ value is 2.0039. Both coupling constants and $\langle g\rangle$ values are clearly indicative of a radical species in which the unpaired electron is mostly localized over the semiquinone ligand.[21,22] In particular, the low A_{Co} coupling constant confirms the presence of Co(III) in a semiquinoid structure.[23] As shown in Figure 4, the experimental and computed spectra slightly disagree, particularly on the wings. This may be attributed to the presence of minor amounts of additional paramagnetic species arising from the chemical complication coupled to the charge transfer.

The two-electron-oxidation product was treated as follows after solvent evaporation. The crude product was extracted twice with diethyl ether; as a result a yellow solution and a yellow brown solid were obtained. The ethereal solution was evaporated to give 3,5-DBQ in 80% yield as revealed by comparison with an authentic specimen. The solid residue, washed with CH_2Cl_2 and ethanol, was characterized by NMR data and elemental analyses as $[(triphos)Co(NCMe)_2](ClO_4)_3$ (**6**) [IR: 2320, 2300 cm^{-1}, coordinated MeCN; 1090, 620 cm^{-1}, ClO_4^-. $^{31}P\{^1H\}$ NMR (CD_3CN, 293 K): 36.20 ppm, triphos. ^1H NMR (CD_3CN, 293 K): 2.15 ppm, multiplet, coordinated CH_3CN. Λ_M(MeCN): 375 Ω^{-1} cm^2 mol^{-1}].

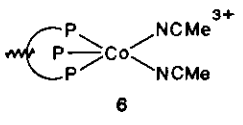

6

Scheme I describes the overall electrode mechanism relative to the anodic oxidation processes. The cathodic system at −0.40 V, which is present in the cyclic voltammograms after the exhaustive two-electron oxidation, is assigned to the Co(III)/Co(II) redox couple in the new solvento complex $[(triphos)Co(NCMe)_2]^{3+}$.

The molecule 3,5-DBQ in MeCN is known to give rise to the redox processes in (11).[24]

$$3,5\text{-DBQ} + e^- \rightleftarrows DBSQ^- \quad E^{\circ\prime} = -0.51 \text{ V}$$

$$3,5\text{-DBQ} + 2H^+ + 2e^- \rightleftarrows H_2DBCat \quad E^{\circ\prime} = +0.40 \text{ V} \qquad (11)$$

Accordingly, the processes at −0.52 and +0.44 V can be attributed to the above reactions. In fact, recall that free quinone forms after the two-electron oxidation. In addition, protons can be provided by the MeCN solvent, which is only formally "anhydrous".

The redox behavior of $[(triphos)Co(o\text{-}Cl_4Cat)]ClO_4$ (**7**) is essentially similar to that of **1**. Interestingly, the one-electron exhaustive cathodic reduction (E_W = −0.5 V) causes the precipitation of **4**, which is sparingly soluble in MeCN. In addition, the electrogenerable semiquinone complex $[(triphos)Co(o\text{-}Cl_4SQ)]^{2+}$ is more stable than the 3,5-DBSQ analogue as shown in Figure 5, which illustrates the cyclic voltammogram recorded after the one-electron exhaustive anodic electrolysis (E_W = +1.1 V).

The semiquinoid nature of this product has been determined by EPR techniques. Owing to the extreme difficulty in assessing all the peaks, it has not been possible to simulate the EPR spectrum. However, the general features of the latter, namely the low coupling constants, the $\langle g\rangle$ factor close to 2.00, and the

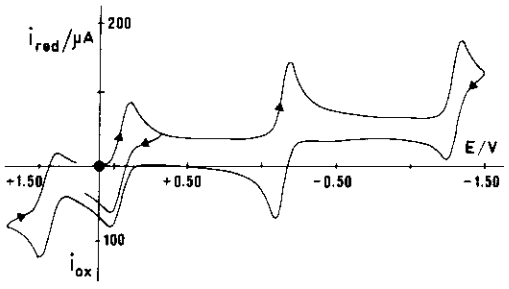

Figure 5. Cyclic voltammogram recorded at a platinum electrode on a MeCN solution containing **7** (1.5×10^{-4} mol) and $[NEt_4ClO_4$ (0.1 mol dm^{-3}) after bulk electrolysis at +1.1 V. Scan rate: 0.2 V s^{-1}. ● indicates starting potential for cyclic scans.

Table II. Standard Electrode Potentials (V vs SCE) for the Redox Changes Observed in MeCN Solutions of the Cobalt(III) Catecholates **1**, **7**, and **8**

compd	$Co^I(Cat)/Co^{II}(Cat)$	$Co^{II}(Cat)/Co^{III}(Cat)$	$Co^{III}(Cat)/Co^{III}(SQ)$	$Co^{III}(SQ)/Co^{III}(Q)$
1	−1.63	−0.49	+0.73	+1.04
7	−1.27	−0.12	+0.98	+1.38
8	−1.58[a]	−0.53	+0.60	+0.79

[a] Peak potential value at 0.2 V s^{-1}.

Scheme I

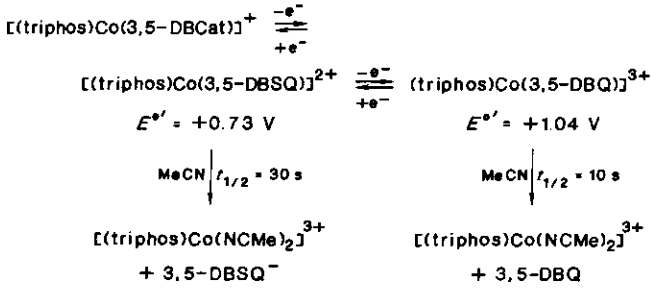

(21) Wicklund, P. A.; Beckmann, L. S.; Brown, D. G. *Inorg. Chem.* **1976**, *15*, 1996.
(22) Pierpont, C. G.; Buchanan, R. M. *Inorg. Chem.* **1982**, *21*, 652.
(23) Brown, D. G.; Hemphill, W. D. *Inorg. Chem.* **1979**, *18*, 2039.
(24) Stallings, M. D.; Morrison, M. M.; Sawyer, D. T. *Inorg. Chem.* **1981**, *20*, 2655.

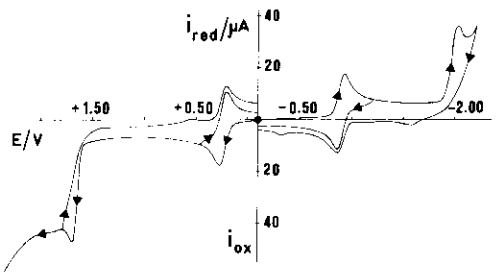

Figure 6. Cyclic voltammogram recorded at a platinum electrode on a MeCN solution containing **5** (9.2×10^{-4} mol dm^{-3}) and $[NEt_4]ClO_4$ (0.1 mol dm^{-3}). Scan rate: 0.2 V s^{-1}. ● indicates starting potential.

spectral range of ca. 70 G, are those expected for a semiquinone radical in the presence of four chlorine, one cobalt, and three phosphorus nuclei. In this respect, recall that the spectrum of the cobalt (II) catecholate derivative spans over ca. 350 G.

Analogously to $[(triphos)Co(3,5\text{-}DBQ)]^{3+}$, the quinone complex $[(triphosCo(o\text{-}Cl_4Q)]^{3+}$ is a transient species.

Finally, $[(triphos)Co(phenCat)]ClO_4$ (**8**) displays an electrode behavior qualitatively similar to those of **1** and **7**. In this case, however, the cobalt(III) semiquinone complex is very unstable.

Table II summarizes the redox potentials for the charge transfers displayed by the catecholate complexes **1**, **7**, and **8**.

The potentials of both the ligand-centered oxidations and the metal-centered reductions reflect the electronic nature of each catechol moiety; i.e., $o\text{-}Cl_4Cat$ is much more electron-withdrawing than 3,5-DBCat, which in turn is more electron-withdrawing than phenCat.

Interestingly, the electrochemical results point out the metal and ligand character for the LUMO/HOMO pair of the cobalt(III) catecholate complexes. Neglecting the solvent effects, a difference of ca. 1.1–1.2 eV between the HOMO and LUMO energies for the three complexes may be computed.

To confirm that the redox behavior of the present series of compounds is characteristic of the quinoid coligands, we have studied the electrochemistry of the tropolonato complex **5**. Figure 6 shows the cyclic voltammogram recorded in MeCN solution. This consists of an uncomplicated one-electron reversible anodic process ($E^{\circ\prime} = +0.23$ V) due to the Co(II)/Co(III) redox couple and of a one-electron reversible cathodic process ($E^{\circ\prime} = -0.90$ V) attributable to the Co(II)/Co(I) redox step. The latter is complicated by subsequent chemical reactions. Both the irreversible oxidation ($E_p = +1.7$ V) and reduction ($E_p = -2.0$ V) processes are most likely due to ligand-centered charge transfers. As a matter of fact, free tropolone in MeCN undergoes an irreversible anodic process at +1.68 V and an irreversible (electrode-poisoning) cathodic process at −1.40 V.

MO Analysis. The chemistry of the present complexes (triphos)CoL (L = *o*-quinone, *o*-semiquinone, catecholate) can be discussed with the help of the interaction diagram of Figure 7 which was constructed by means of extended Hückel (EHMO)[25] and fragment molecular orbital (FMO)[26] calculations.

The model used for the L_3M type of fragment is highly simplified since the terminal phosphine ligands have been replaced with hydrides and the molecular charges adjusted to formally reproduce all of the members of the redox series (triphos)CoL^n ($n = +3, +2, +1, 0, -1$). In addition, all the C–C distances within the six-membered ring were kept equal to 1.4 Å in order to avoid biasing of the overlap population analysis when different members of the series are compared. At the left of the diagram the frontier orbitals of a L_3M fragment with C_{3v} symmetry are reported. The features of these FMOs have been illustrated innumerable times.[27] Here it is sufficient to point out that two of the three higher orbitals (excluding the lower three d orbitals of the "t_{2g}" set) are used for

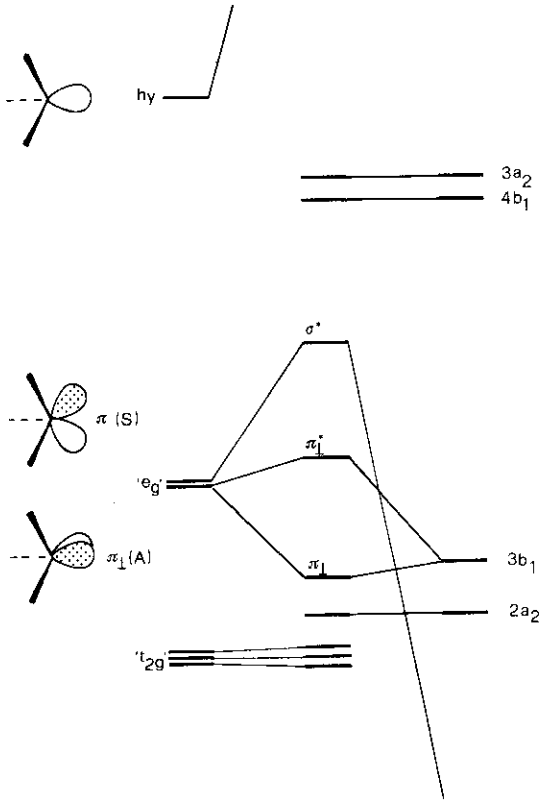

Figure 7. Diagram for some of the interactions between the fragment molecular orbitals of a L_3Co group and those of a $H_4C_6O_2$ *o*-quinoid ligand. The labels S and A refer to FMOs symmetric or antisymmetric with respect to the plane of the drawing.

σ bonding with the chelate L. In fact, two σ-bonding interactions, VII and VIII, involve the metal high-lying σ hybrid (hy) and the

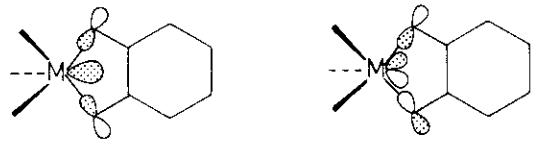

VII VIII

S member of the "e_g" set, which has π symmetry in the plane of the chelate. The ligand uses two low-lying combinations of oxygen lone pairs with proper in-phase and out-of-phase symmetry. Only one σ^* interaction (the antibonding one corresponding to VIII) falls inside the diagram of Figure 7.

The plane of the metallacycle Co–O–C–C–O is a node for the A member of the "e_g" set. The latter $\pi_\perp$ metal FMO interacts somewhat with members of the $\pi_\perp$ system (IX) of the planar

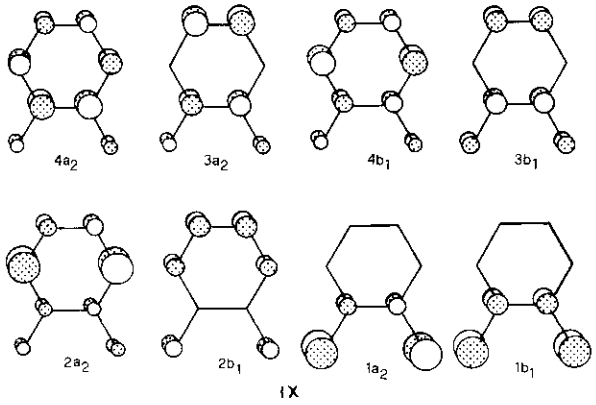

IX

ligand $H_4C_6O_2$, and some of the interactions account for the peculiar redox features of the compounds. The eight non-hydrogen atoms of the ligand contribute one p_π orbital each. For the

(25) (a) Hoffmann, R.; Lipscomb, W. N. *J. Chem. Phys.* **1962**, *36*, 2179, 3489; **1962**, *37*, 2872. (b) Hoffmann, R. *Ibid.* **1963**, *39*, 1397.
(26) Fujimoto, H.; Hoffmann, R. *J. Chem. Phys.* **1964**, *78*, 1167.
(27) Albright, T. A.; Burdett, J. K.; Whangho, M. H. *Orbital Interactions in Chemistry*; Wiley: New York, 1975.

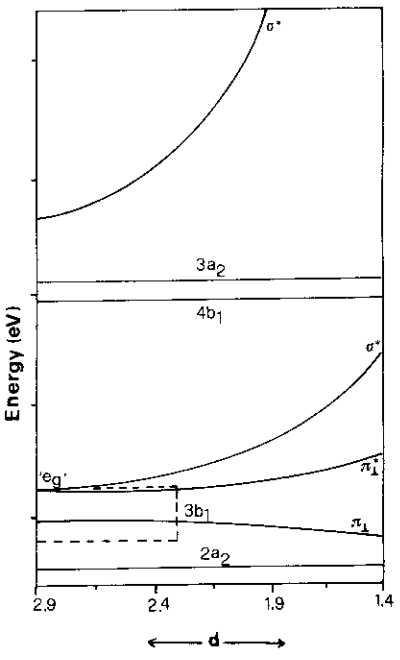

Figure 8. Evolution of some relevant frontier MOs for approaching together a L_3Co fragment and a *o*-quinone molecule along a least-motion pathway (defined in XII).

o-quinone molecule the lower four symmetry combinations (second row in IX) are populated. Although two of the lowest MOs are strongly centered on the oxygen atoms, their overall C–O nature is bonding, so that the whole picture is consistent with four double bonds in the molecule, as it appears in the VB description I.

In agreement with previous calculations,[7] the quinone's LUMO ($3b_1$) has C–O antibonding character but also C–C bonding character. Such a MO lies at an energy low enough to be easily populated as it occurs in catecholate. Our calculation establishes the HOMO–LUMO energy gap at ca. 0.6 eV in *o*-benzoquinone, the HOMO being the π $2a_2$ level. The gap is likely too small to be consistent with the stability of the free molecule. An optimization of the geometry, not attempted by us, may possibly increase the energy gap, but this is not essential for the development of our qualitative arguments.

On account of a poor overlap the bonding and antibonding MOs resulting from the interaction $3b_1$ (*o*-quinone)–$\pi_\perp$(A) (metal) levels do not largely diverge from the energies of their parent FMOs. The lower MO is one largely centered on the ligand and the higher on the metal. The calculated energy gap is slightly larger than 1 eV, which is quite consistent with the gap derivable from electrochemical data. The nature and the frontier location of these bonding/antibonding $\pi_\perp$ MOs can be easily related to the chemical, structural, and electrochemical information presented in the previous paragraphs. First of all, in the cobalt (III) catecholate complex, two electrons populate the bonding MO X (HOMO).

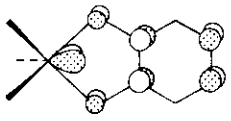

X

The contribution of the metal is exaggerated here as 92% of this MO has quinone's character; nonetheless, the MO is Co–O bonding, C–O antibonding, and C–C bonding. This accounts for the π delocalization within the Co–O–C–C–O metallocycle that is transparent in the crystal structure analysis. It is worth pointing out that, although small, the contribution of the metal to the HOMO has some important consequences. Thus, the complex cannot be exactly defined a 16-electron species because the metal $\pi_\perp$(A) level accepts part of the electron density located in the ligand's $3b_1$ FMO. By virtue of such a donor/acceptor interaction the ligand's level is not fully populated as in the free catecholate anion. A comparison of the calculated overlap populations for free catecholate and quinone groups is shown in XI. A certain

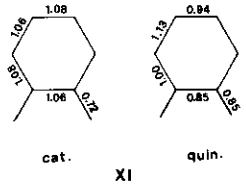

XI

elongation of the C_{12}–C_{13}, C_{11}–C_{16}, and C_{14}–C_{15} bonds in **2** (refer to Figure 1 and Table I) is indicative of an effective charge delocalization toward the metal, the ligand assuming an incipient quinone character.

The next important question concerns the origin of the two electrons populating the HOMO of the complex. It is worth recalling that in reaction 1 the two interacting fragments, (triphos)Co(II) and 3,5-DBQ, carry initially one electron distributed over the two members of the metal "e_g" set and none in the quinone $3b_1$ level.

Assuming a least-motion pathway in the complex formation (XII), the two orbitals smoothly begin to interact with each other and correlate with the complex HOMO ($\pi_\perp$) and LUMO ($\pi_\perp$*), respectively. This is clearly indicated by the Walsh diagram of Figure 8.

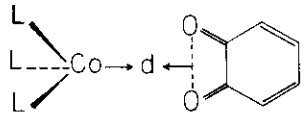

XII

The metal unpaired electron in the "e_g" level, which is destined to become $\pi_\perp$*, can greatly lower its energy by jumping into the lower $\pi_\perp$ level. Since both levels have the same (A) symmetry they immediately begin to "feel" each other along the pathway (boxed region). As pointed out for other organometallic reactions involving electron-transfer mechanisms,[28] the transformation *o*-quinone/catecholate can be achieved through metal to ligand *electron jumping* allowed by MO mixing in an *avoided-crossing* region.[29] Thermodynamic stability may be achieved by fully populating the bonding $\pi_\perp$ level, which lies at low energy. Thus, it is not strange that **1**, the easily isolated product, is diamagnetic with an extra electron with respect to the total electron count of the reagents. The origin of this extra electron is unknown, but it can be reasonably hypothesized that it comes from the alcohol in solution. On the other hand, the species with only one unpaired electron in the $\pi_\perp$ level has a finite lifetime as shown by the ease of electrochemical oxidation of **1** and its characterization by EPR techniques. The latter data are fully consistent with the assignment of the unpaired electron to the ligand (semiquinone species) and hence with the MO calculations.

The two-electron oxidation of **1** is also electrochemically feasible but complicated by subsequent chemical reactions. In particular, the chelate ligand, which becomes pure *o*-quinone upon oxidation, may be easily displaced by two CH_3CN solvent molecules. Also, the high instability of the *o*-quinone complex of Co(III) is easily rationalized in MO terms as the HOMO–LUMO gap for such a species would be very small (see Figure 8). Moreover, the *o*-quinone ligand is not an electron-rich molecule and is unable to fullfil the high need for electrons of (triphos)Co(III), a d^{12} species. Notice that the metal "e_g" (A) level, relatively low in energy, would not be engaged in any donor–acceptor interaction with the ligand.

The interaction diagram of Figure 8 also explains the behavior of the complex **1** upon chemical or electrochemical reduction. The

(28) (a) Bianchini, C.; Mealli, C.; Meli, A.; Sabat, M.; Zanello, P. *J. Am. Chem. Soc.* **1987**, *109*, 185. (b) Mealli, C.; Sabat, M.; Marzilli, L. G. *Ibid.* **1987**, *109*, 1593.

(29) Salem, L. *Electrons in Chemical Reactions: First Principles*; Wiley-Interscience: New York, 1982.

$\pi_\perp$* level lies at an energy accessible for population. The metal-centered nature of this MO is clearly consistent with EPR data relative to those of the cobalt(II)catecholate species, **4**. The metal–ligand antibonding nature of the SOMO greatly reduces the interaction between the two fragments and possibly the extra stability due to the $\pi_\perp$ delocalization through the metallocycle. For this reason a two-electron reduction leads to a Co(I) product that has a very short lifetime. Also notice that a σ* level lies not too higher than the $\pi_\perp$* MO; hence, second-order Jahn–Teller effects that lead to the disruption of the main square-pyramidal framework are possible.

The one-electron-reduced complex is directly comparable with the only species obtainable from (triphos)Co(II) and the anion tropolonate. At this point an interesting question may be raised concerning the lack of redox chemistry for tropolonate complexes. A similar difference between the complexes of bis(dithiolene) and bis(dithiotropolonato) ligands was already pointed out.[30] VB and MO viewpoints were used by Khare, Schultz, and Eisenberg[31] to compare dithiotropolonate and benzene-1,2-dithione models. Here, we endeavor to analyze again the problem to offer a qualitative explanation for the different nature of six- and seven-membered carbon cycles substituted in ortho positions by two calchogen atoms.

In the catecholate dianion the aromaticity of the C_6 ring is only slightly perturbed by the two oxygen atoms. As shown in XIII,

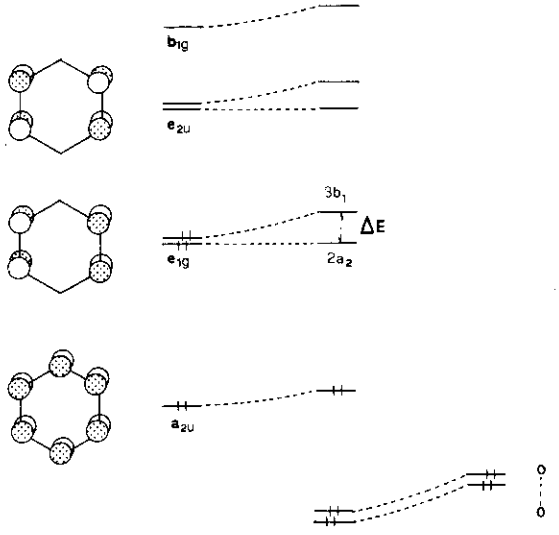

XIII

two of the six benzene π levels interact mostly with in-phase and out-of-phase combinations of oxygen π orbitals. Both ring levels will be destabilized in antibonding fashion. One member of the e_{2u} level is empty and remains empty. One member of the lower e_{1g} set is pushed up by the in-phase combination of oxygen orbitals. The degenerate members are forced to split. Depending on the magnitude of the split, the destabilized level ($3b_1$ in IX) may or may not be depopulated. Notice that the two electrons eventually removed, out of a total of 10, are essential to the aromaticity of the C_6 ring. The MO arguments confirm the lack of aromaticity implicit in *o*-quinone. The latter is better described in terms of *pericyclic topology*[32] as a open butadiene ribbon closed by a O=C—C=O fragment. Although the molecule is planar, the π system is practically separated in two parts. Interestingly, upon complexation to a metal, the important frontier orbital remains the one that, occupied or not, determines the aromaticity of the C_6 ring. This level is even slightly stabilized by the interaction with the metal $\pi_\perp$ level, but within the complex, the reversible transformation quinone/catecholate may essentially occur with the same ease as within the free ligand.

Analogous trends are in first approximation found for the ligand tropolonate. The perturbation brought about by two ortho oxygen atom on the aromatic tropylium ($C_7H_7^+$) cation[33] has similar effects. One empty (XIV) and one filled (XV) ring combination are destabilized.

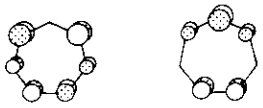

XIV XV

A calculation shows that similar to the previous case a ΔE gap (0.6 eV) between the members of an initially degenerate and populated set can in principle favor the removal of two electrons from the tropolonato anion. The energetics of the EHMO method cannot say too much about the relative stability of the hypothetical resulting carbocation XVI.

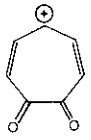

XVI

However, we find an important key that excludes the possibilities for an easy redox chemistry. In fact, the filled degenerate π-bonding levels of tropylium are somewhat lower in energy than the corresponding benzene MOs (e_{1g} in XIII). In particular the first degenerate π set is ca. 0.5 eV lower in $C_7H_7^+$ than in the corresponding C_6H_6 ring and lies in the same energy region as some σ levels. Although one member of the degenerate π level (XV) is destabilized by the oxygen atoms, it cannot be precisely established whether the HOMO of tropolonate has π symmetry or not. At the EHMO level it depends on the C–O distances used in the calculations whether a π level is the HOMO or the second HOMO. In any case, the removal of two electrons from the system will be a source of molecular instability given the absence of a HOMO–LUMO gap. In metal complexes the situation is perfectly analogous: upon abstraction of two electrons there is an insufficient HOMO–LUMO gap and hence a source of instability. The differences between the chemistry of catecholate and troponolate complexes can be framed within these simple MO arguments.

Conclusions. The present study has illustrated the genesis and the nature of a series of complexes that, on account of their unique chemical and structural composition, may exist as electronic isomers. Although this is not novel for complexes of the noninnocent *o*-quinoid ligands, the information gathered on the nature of each single product and the possibilities of redox transformations between the different members of the series have been widely explored. The qualitative MO arguments provide simple keys for the understanding of the whole system, including synthetic routes to many products. Also, it seems particularly educational to note the comparison between similarly structured ligands that only differ for the size of the ring ortho-substituted by oxygen atoms, namely catecholate and tropolonate. Again, by the use of qualitative MO arguments, a rationale for the lack of redox properties of the latter ligand and its complexes can be provided.

Experimental Section

General Information. All reactions and manipulations were carried out under a nitrogen atmosphere. Reagent grade chemicals were used in the preparations of the complexes. The solid complexes were collected on sintered-glass frits and washed with appropriate solvents before being dried in a stream of nitrogen. Infrared spectra were recorded with a Perkin-Elmer 475 grating spectrophotometer on samples mulled in Nujol between KBr plates. ^1H and $^{31}P\{^1H\}$ NMR spectra were taken with a Varian CFT 20 spectrometer. Peak positions are relative to tetramethylsilane and phosphoric acid, respectively, with downfield values

(30) Roehrscheid, F.; Balch, A. L.; Holm, R. H. *Inorg. Chem.* **1966**, *5*, 1542.
(31) Khare, G. P.; Schultz, A. J.; Eisenberg, R. *J. Am. Chem. Soc.* **1971**, *93*, 3597.
(32) Goldstein, M. J.; Hoffmann, R. *J. Am. Chem. Soc.* **1971**, *93*, 6193.
(33) Yates, K. *Hückel Molecular Orbital Theory*; Academic: New York, 1978; p 139.

reported as positive. Conductance measurements were made with a WTW Model LBR/B conductivity bridge. Ultraviolet–visible spectra were recorded on a Beckman DK-2A spectrophotometer. Magnetic susceptibilities of solid samples were measured on a Faraday balance. The materials and the apparatus used for the electrochemical experiments have been described elsewhere.[28a] The potential values are relative to an aqueous calomel electrode (SCE). The temperature was controlled at 20 ± 0.1 °C. Under the present experimental conditions the ferrocenium/ferrocene couple was located at +0.38 V. X-Band EPR spectra were recorded with an ER 200-SRCB Bruker spectrometer operating at w_0 = 9.78 GHz. The control of the external magnetic field was obtained with a microwave bridge ER 041 MR Bruker wavemeter. The temperature was varied and controlled with an ER 4111 VT Bruker device with an accuracy of ±1 K. In order to estimate accurate g_{iso} and g_{aniso} values over the temperature range of interest, the diphenylpicrylhydrazyl (DPPH) free radical was used as field maker (g_{iso}DPPH = 2.0036, w_0 = 9.43 GHz). To avoid Co dipole–dipole interactions in frozen and room-temperature solutions, low concentrations were used (less than 10^{-3} M). In order to assure quantitative reproducibility, the samples were placed into calibrated quartz capillary tubes permanently positioned in the resonance cavity.

Synthesis of [(triphos)Co(3,5-DBCat)]ClO_4 (1). Method 1. To azeotrope off the water of the perchlorate salt, a solution of $Co(ClO_4)_2 \cdot 6H_2O$ (0.36 g, 1 mmol) in 1-butanol (100 mL) was gently concentrated by heating at boiling temperature to ca. 5 mL. Triphos (0.62 g, 1 mmol) in CH_2Cl_2 (10 mL) was then added. The resulting light orange solution turned blue by treatment with 3,5-DBQ (0.22 g, 1 mol) in CH_2Cl_2 (10 mL). Addition of a 1:3 mixture of ethanol/diethyl ether (40 mL) led to the precipitation of blue crystals, which were filtered off and washed with diethyl ether; yield 80%. Anal. Calcd for $C_{55}H_{59}ClCoO_6P_3$: C, 65.85; H, 5.93; Co, 5.87. Found: C, 65.71; H, 5.85; Co, 5.79. *Caution!* To avoid detonation of $Co(ClO_4)_2$, the solution must not be taken to near dryness nor should solid material be allowed to deposit on the walls of the reaction flask. It is recommended that work be done behind a protective barrier.

Method 2. A solution (0.5 mmol mL^{-1}) of Na_2(3,5-DBCat) in ethanol (1.1 mL), obtained by reacting catechol with a sodium ethoxide solution in ethanol, was added dropwise to a stirred solution of $[(triphos)Co(\mu\text{-}Cl)_2)Co(triphos)](ClO_4)_2$ (0.41 g, 0.25 mmol) in CH_2Cl_2 (30 mL). During the addition the color changed from red orange to blue, and blue crystals precipitated on elution with diethyl ether (30 mL). They were collected and washed as above; yield 80%.

Method 3. 3,5-DBQ (0.22 g, 1 mmol) was added to a mixture of $Co_2(CO)_8$ (0.17 g, 0.5 mmol) and triphos (0.62 g, 1 mmol) in THF (40 mL). On addition of $(NBu_4)ClO_4$ (0.34 g, 1 mmol) in ethanol (10 mL) to the resulting deep violet solution there was an immediate color change to blue. Blue crystals separated by elution with diethyl ether (40 mL). They were filtered off and washed as above; yield 80%. Crystals of formula $[(triphos)Co(3,5\text{–}DBCat)]BPh_4 \cdot 0.5C_4H_9OH \cdot C_2H_5OH$ (2) suitable for x-ray analysis were obtained by methatetical reaction of **1** with $NaBPh_4$ in CH_2Cl_2/ethanol/1-butanol. Anal. Calcd for $C_{83}H_{90}BCoO_{3.5}P_3$: C, 76.32; H, 6.95; Co, 4.51. Found: C, 76.17, H, 7.00; Co, 4.36.

Synthesis of [(triphos)Co(Cat)]ClO_4 [Cat = *o*-Cl_4Cat (7), phenCat (8)]. These compounds (green and violet in color, respectively) were prepared by following the above three methods by using the appropriate *o*-quinone. Metathetical reaction with $NaBPh_4$ in CH_2Cl_2/ethanol gave the corresponding tetraphenylborate salts.

Synthesis of (triphos)Co(3,5-DBCat) (3). Method 1. 3,5-DBQ (0.22 g, 1 mmol) was added to a mixture of $Co_2(CO)_8$ (0.17 g, 0.5 mmol) and triphos (0.62 g, 1 mmol) in THF (40 mL). There was an immediate color change from red brown to violet. On elution with *n*-pentane (80 mL) compound **3** precipitated as a brown violet powder that was filtered off and washed with *n*-pentane; yield 70%.

Method 2. A solution of $Co(Cp)_2$ (0.07 g, 0.35 mmol) in MeCN (10 mL) was added dropwise to a stirred solution of **1** (0.3 g, 0.3 mmol) in MeCN (10 mL) producing a violet solution. A violet powder precipitated on standing within 2 h. This was filtered off and washed with a 1:1 mixture of MeCN/*n*-butyl ether and *n*-pentane; yield 85%. Anal. Calcd for $C_{55}H_{59}CoO_2P_3$: C, 73.08; H, 6.57; Co, 6.51. Found: C, 72.83; H, 6.49; Co, 6.41.

Synthesis of (triphos)Co(*o*-Cl_4Cat) (4). The compound was prepared as orange brown crystals by following the above two methods as for **3** except for the substitution of *o*-Cl_4Q and **8** for 3,5-DBQ and **1**, respectively. Anal. Calcd for $C_{47}H_{39}Cl_4CoO_2P_3$: C, 60.73; H, 4.22; Co, 6.34. Found: C, 60.83; H, 4.13; Co, 6.28. Powder EPR (298 K): broad resonance with $\langle g \rangle$ = 2.11. Solution EPR (CH_2Cl_2, 290 K): two species with $\langle g_1 \rangle$ = 2.11 ($\langle A_{Co} \rangle$ = 45 × 10^{-4} cm^{-1}) and $\langle g_2 \rangle$ = 2.12 ($\langle A_{Co} \rangle$ = 44 × 10^{-4} cm^{-1}). Frozen solution EPR (CH_2Cl_2, 100 K): one species with g_1 = 2.20 (A_{Co} = 74 × 10^{-4} cm^{-1}), $g_2 \simeq$ 2.08 (A_{Co} = 60 × 10^{-4} cm^{-1}), and g_3 = 1.97 (A_{Co} = 53 × 10^{-4} cm^{-1}).

Table III. Summary of Crystal Data

formula	$C_{83}H_{90}P_3BCoO_{3.5}$
mol wt	1306.31
cryst form	parallelepiped
cryst size, mm	0.575 × 0.175 × 0.05
space group	$P2_1/a$
a, Å	45.940 (8)
b, Å	19.945 (5)
c, Å	16.943 (4)
β, deg	98.94 (3)
V, Å^3	14 566.44
Z	8
d_{calcd}, g cm^{-3}	1.19
μ(Cu Kα), cm^{-1}	20.86
radiation	graphite-monochromated Cu Kα (λ = 1.5418 Å)
2θ range, deg	6–130
scan width, deg	0.8
scan speed, deg s^{-1}	0.04
tot. no. of data	19 488
no. of unique data with $I \geq 3\sigma(I)$	5028
no. of params	532
R	0.078
R_w	0.087

Synthesis of [(triphos)Co($O_2C_7H_5$)]ClO_4 (5). A solution of $Co(ClO_4)_2 \cdot 6H_2O$ (0.36 g, 1 mmol) in 1-butanol (100 mL), from which water was eliminated as described in the synthesis of **1**, was treated with triphos (1.24 g, 2 mmol) in CH_2Cl_2 (10 mL). Tropolone (0.12 g, 1 mmol) in CH_2Cl_2 (10 mL) was added to the resulting solution, which immediately turned from light orange to green. Addition of a 1:3 mixture of ethanol/diethyl ether (40 mL) led to the precipitaton of green crystals, which were filtered off and washed with diethyl ether; yield 85%. Anal. Calcd for $C_{48}H_{44}ClCoO_6P_3$: C, 63.69; H, 5.01; Co, 6.51. Found: C, 63.61; H, 5.11; Co, 6.43. Powder EPR (298 K): broad resonance with $\langle g \rangle$ = 2.08. Solution EPR (MeCN, 290 K): two species with $\langle g_1 \rangle$ = 2.10 ($\langle A_{Co} \rangle$ = 39 × 10^{-4} cm^{-1}) and $\langle g_2 \rangle$ = 2.12 ($\langle A_{Co} \rangle$ = 40 × 10^{-4} cm^{-1}). Frozen solution EPR (CH_2Cl_2, 100 K): one species with g_1 = 2.20 (A_{Co} = 62 × 10^{-4} cm^{-1}), $g_2 \simeq$ 2.08 (A_{Co} = 60 × 10^{-4} cm^{-1}), and g_3 = 1.97 (A_{Co} = 55 × 10^{-4} cm^{-1}).

X-ray Data Collection and Structure Determination. Crystal and intensity data are reported in Table III. X-ray measurements were performed on a Philips PW 1100 diffractometer. The cell constants and orientation matrix were determined by least-squares refinement of the setting angles for 19 reflections. The Cu Kα radiation was purposefully selected given the very long a axis of the cell. The intensities of three standard reflections were measured every 120 min of x-ray exposure. No decay with time was noted. The data were corrected for Lorentz and polarization effects. An empirical correction for the absorption effect was made by using the program DIFABS.[34] The maximum and minimum coefficients ranged between 0.99 and 0.91°. Atomic scattering factors were those tabulated by Cromer and Waber[35] with anomalous dispersion corrections taken from ref 36. The computational work was essentially performed by using the SHELX76 system.[37] The structure was solved by a combination of Patterson and direct-method techniques. A series of F_o Fourier syntheses allowed the location of all the non-hydrogen atoms. During the least-squares refinement rigid-body models (D_{6h} symmetry) were adopted for all the phenyl rings with the C–C distances fixed at 1.39 Å. Anisotropic thermal parameters were used for cobalt and phosphorus atoms. The hydrogen atoms were included at calculated positions (C–H = 1.08 Å). A ΔF map at a late stage of refinement showed some peaks that were attributed to ethanol and 1-butanol solvent molecules. The weakness of the peaks relative to the latter molecule as well as the data of the elemental analysis suggested that the solvent molecules did not have an integer stoichiometry. Accordingly, a population parameter of 0.5 was assigned to the corresponding atoms. The final ΔF map was essentially featureless except for some peaks <1 e/Å^3 in the regions of the solvent molecules, clearly affected by disorder. Atomic coordinates are given in Table IV.

(34) Walker, N.; Stuart, D. *Acta Crystallogr., Sect. A: Found. Crystallogr.* **1983**, *A39*, 158.
(35) Cromer, D. T.; Waber, J. T. *Acta Crystallogr.* **1965**, *18*, 104.
(36) *International Tables of Crystallography*; Kynoch: Brirmingham, England, 1974; Vol. 4.
(37) Sheldrick, G. M. "SHELX76, Program for Crystal Structure Determinations"; University of Cambridge: Cambridge, England, 1976.

Table IV. Final Positional Parameters for the Atoms of [(triphos)Co(3,5-DBCat)]BPh_4·0.5C_4H_9OH·C_2H_5OH[a]

atom	x	y	z	atom	x	y	z	atom	x	y	z
Co_{1a}	1360 (1)	1801 (1)	5181 (2)	$C_{6.6}$	1680 (3)	540 (7)	6635 (8)	C_{512}	3515 (2)	−913 (6)	11252 (8)
P_{1a}	1004 (1)	1917 (2)	5959 (3)	Co_{1b}	3749 (1)	505 (1)	9945 (2)	C_{612}	3303 (2)	−483 (6)	10828 (8)
P_{2a}	1053 (1)	1930 (2)	4001 (3)	P_{1b}	3436 (1)	387 (2)	8767 (3)	B_1	438 (5)	7827 (11)	4704 (15)
P_{3a}	1283 (1)	709 (2)	5129 (3)	P_{2b}	3414 (1)	392 (2)	10770 (3)	C_{113}	362 (2)	6983 (6)	4665 (8)
O_{1a}	1539 (2)	2618 (5)	5551 (7)	P_{3b}	3670 (1)	1590 (2)	9922 (3)	C_{213}	74 (2)	6743 (6)	4530 (8)
O_{2a}	1721 (2)	1605 (6)	4865 (7)	O_{1b}	3930 (2)	−317 (5)	9755 (6)	C_{313}	20 (2)	6055 (6)	4540 (8)
C_{1a}	652 (3)	1552 (8)	5458 (10)	O_{2b}	4103 (2)	691 (5)	10603 (7)	C_{413}	255 (2)	5606 (6)	4684 (8)
C_{2a}	724 (4)	1398 (9)	3887 (11)	C_{1b}	3067 (3)	749 (8)	8850 (10)	C_{513}	544 (2)	5846 (6)	4820 (8)
C_{3a}	898 (4)	453 (9)	5010 (12)	C_{2b}	3077 (3)	903 (8)	10425 (10)	C_{613}	598 (2)	6534 (6)	4810 (8)
C_{4a}	661 (4)	1058 (9)	4751 (11)	C_{3b}	3280 (3)	1815 (8)	9542 (10)	C_{114}	372 (3)	8143 (5)	5598 (8)
C_{5a}	367 (4)	705 (9)	4543 (11)	C_{4b}	3048 (4)	1257 (8)	9541 (11)	C_{214}	190 (3)	7828 (5)	6097 (8)
C_{11a}	1809 (4)	2688 (9)	5347 (11)	C_{5b}	2744 (4)	1572 (9)	9383 (11)	C_{314}	143 (3)	8121 (5)	6852 (8)
C_{12a}	1907 (4)	2139 (9)	4927 (12)	C_{11b}	4197 (3)	−384 (8)	10198 (9)	C_{414}	278 (3)	8730 (5)	7108 (8)
C_{13a}	2182 (4)	2095 (9)	4617 (12)	C_{12b}	4292 (4)	173 (8)	10668 (10)	C_{514}	460 (3)	9045 (5)	6609 (8)
C_{14a}	2357 (4)	2665 (9)	4764 (11)	C_{13b}	4566 (4)	220 (9)	11223 (11)	C_{614}	507 (3)	8752 (5)	5854 (8)
C_{15a}	2265 (4)	3242 (9)	5200 (12)	C_{16b}	4749 (4)	−331 (9)	11180 (11)	C_{115}	102 (2)	8824 (6)	3915 (7)
C_{16a}	1999 (4)	3270 (9)	5503 (11)	C_{15b}	4656 (4)	−918 (9)	10705 (11)	C_{215}	197 (2)	8163 (6)	3860 (7)
C_{17a}	2662 (4)	2681 (11)	4427 (14)	C_{14b}	4389 (4)	−951 (8)	10195 (10)	C_{315}	118 (2)	8702 (6)	3116 (7)
C_{18a}	1907 (4)	3875 (10)	5959 (13)	C_{18b}	4283 (4)	−1576 (10)	9677 (13)	C_{415}	−55 (2)	8103 (6)	2427 (7)
C_{19a}	2632 (5)	2313 (13)	3570 (17)	C_{17b}	5056 (4)	−355 (10)	11729 (12)	C_{515}	−149 (2)	8764 (6)	2482 (7)
C_{20a}	2760 (6)	3427 (15)	4240 (18)	C_{22b}	4556 (4)	−2106 (10)	9687 (13)	C_{615}	−70 (2)	9125 (6)	3226 (7)
C_{21a}	2891 (6)	2311 (15)	5076 (20)	C_{23b}	4198 (4)	−1381 (10)	8730 (13)	C_{116}	780 (3)	7974 (6)	4546 (7)
C_{22a}	1798 (4)	3673 (10)	6817 (13)	C_{24b}	4015 (4)	−1915 (10)	10030 (12)	C_{216}	1007 (3)	4820 (6)	5198 (7)
C_{23a}	1657 (4)	4231 (9)	5370 (12)	C_{19b}	5286 (4)	−410 (11)	11081 (13)	C_{316}	1299 (3)	7957 (6)	5111 (7)
C_{24a}	2173 (4)	4388 (10)	6224 (13)	C_{20b}	5125 (5)	320 (13)	12244 (16)	C_{416}	1363 (3)	8247 (6)	4372 (7)
$C_{1.1}$	1101 (2)	1491 (5)	6959 (8)	C_{21b}	5085 (4)	−994 (11)	12318 (14)	C_{516}	1136 (3)	8400 (6)	3719 (7)
$C_{2.1}$	1344 (2)	1752 (5)	7488 (8)	$C_{1.7}$	3350 (3)	9553 (5)	8298 (7)	C_{616}	844 (3)	8264 (6)	3806 (7)
$C_{3.1}$	1435 (2)	1465 (5)	8276 (8)	$C_{2.7}$	3222 (3)	9518 (5)	7455 (7)	B_2	3012 (4)	4364 (10)	−466 (13)
$C_{4.1}$	1282 (2)	918 (5)	8536 (8)	$C_{3.7}$	3135 (3)	8899 (5)	7094 (7)	C_{117}	2843 (3)	4114 (4)	337 (8)
$C_{5.1}$	1039 (2)	657 (5)	8007 (8)	$C_{4.7}$	3177 (3)	8316 (5)	7576 (7)	C_{217}	2687 (3)	4552 (4)	779 (8)
$C_{6.1}$	948 (2)	943 (5)	7219 (8)	$C_{5.7}$	3305 (3)	8352 (5)	8420 (7)	C_{317}	2547 (3)	4311 (4)	1428 (8)
$C_{1.2}$	903 (3)	2746 (6)	6314 (8)	$C_{6.7}$	3392 (3)	8970 (5)	8781 (7)	C_{417}	2563 (3)	3631 (4)	1635 (8)
$C_{2.2}$	737 (3)	2775 (6)	6968 (8)	$C_{1.8}$	3566 (3)	801 (5)	7896 (7)	C_{517}	2720 (3)	3193 (4)	1192 (8)
$C_{3.2}$	659 (3)	3395 (6)	7269 (8)	$C_{2.8}$	3833 (3)	565 (5)	7695 (7)	C_{617}	2860 (3)	3434 (4)	543 (8)
$C_{4.2}$	747 (3)	3986 (6)	6917 (8)	$C_{3.8}$	3961 (3)	879 (5)	7067 (7)	C_{118}	2881 (3)	5127 (6)	−819 (8)
$C_{5.2}$	914 (3)	3956 (6)	6263 (8)	$C_{4.8}$	3823 (3)	1431 (5)	6641 (7)	C_{218}	2696 (3)	5200 (6)	−1587 (8)
$C_{6.2}$	992 (3)	3336 (6)	5962 (8)	$C_{5.8}$	3557 (3)	1667 (5)	6842 (7)	C_{318}	2600 (3)	5836 (6)	−1867 (8)
$C_{1.3}$	923 (2)	2786 (6)	3956 (7)	$C_{6.8}$	3428 (3)	1352 (5)	7469 (7)	C_{418}	2689 (3)	6400 (6)	−1379 (8)
$C_{2.3}$	642 (2)	2996 (6)	3962 (7)	$C_{1.9}$	3896 (3)	2069 (5)	9310 (8)	C_{518}	2874 (3)	6326 (6)	−610 (8)
$C_{3.3}$	567 (2)	3673 (6)	3884 (7)	$C_{2.9}$	4133 (3)	1766 (5)	9011 (8)	C_{618}	2970 (3)	5690 (6)	−330 (8)
$C_{4.3}$	773 (2)	4141 (6)	3699 (7)	$C_{3.9}$	4316 (3)	2146 (5)	8580 (8)	C_{119}	2962 (2)	3800 (6)	−1234 (8)
$C_{5.3}$	1055 (2)	3931 (6)	3594 (7)	$C_{4.9}$	4263 (3)	2829 (5)	8448 (8)	C_{219}	3197 (2)	3570 (6)	−1612 (8)
$C_{6.3}$	1130 (2)	3254 (6)	3672 (7)	$C_{5.9}$	4026 (3)	3132 (5)	8747 (8)	C_{319}	3148 (2)	3099 (6)	−2259 (8)
$C_{1.4}$	1189 (2)	1751 (6)	2994 (8)	$C_{6.9}$	3842 (3)	2753 (5)	9178 (8)	C_{419}	2864 (2)	2859 (6)	−2529 (8)
$C_{2.4}$	980 (2)	1732 (6)	2267 (8)	C_{110}	3756 (2)	2018 (6)	10928 (8)	C_{519}	2629 (2)	3089 (6)	−2152 (8)
$C_{3.4}$	1067 (2)	1609 (6)	1489 (8)	C_{210}	3544 (2)	2241 (6)	11398 (8)	C_{619}	2678 (2)	3559 (6)	−1504 (8)
$C_{4.4}$	1364 (2)	1506 (6)	1437 (8)	C_{310}	3631 (2)	2559 (6)	12169 (8)	C_{120}	3380 (3)	4445 (5)	−133 (7)
$C_{5.4}$	1574 (2)	1525 (6)	2164 (8)	C_{410}	3930 (2)	2654 (6)	12470 (8)	C_{220}	3546 (3)	4855 (5)	−583 (7)
$C_{6.4}$	1486 (2)	1648 (6)	2942 (8)	C_{510}	4142 (2)	2431 (6)	12000 (8)	C_{320}	3852 (3)	4880 (5)	−365 (7)
$C_{1.5}$	1436 (2)	298 (6)	4284 (8)	C_{610}	4055 (2)	2113 (6)	11229 (8)	C_{420}	3992 (3)	4494 (5)	303 (7)
$C_{2.5}$	1272 (2)	155 (6)	3499 (8)	C_{111}	3505 (2)	607 (6)	11879 (7)	C_{520}	3826 (3)	4083 (5)	753 (7)
$C_{3.5}$	1413 (2)	−89 (6)	2852 (8)	C_{211}	3798 (2)	700 (6)	12239 (7)	C_{620}	3520 (3)	4059 (5)	535 (7)
$C_{4.5}$	1717 (2)	−190 (6)	2991 (8)	C_{311}	3868 (2)	881 (6)	13084 (7)	C_{25}	2548 (3)	3259 (8)	3018 (10)
$C_{5.5}$	1881 (2)	−48 (6)	3776 (8)	C_{411}	3644 (2)	970 (6)	13568 (7)	C_{26}	2503 (7)	5897 (17)	3435 (22)
$C_{6.5}$	1740 (2)	197 (6)	4422 (8)	C_{511}	3351 (2)	877 (6)	13208 (7)	C_{27}	2349 (4)	5377 (10)	4286 (12)
$C_{1.6}$	1457 (3)	257 (7)	6053 (8)	C_{611}	3281 (2)	696 (6)	12364 (7)	C_{28}	334 (22)	323 (55)	1700 (72)
$C_{2.6}$	1371 (3)	−406 (7)	6149 (8)	C_{112}	3033 (2)	−736 (6)	10440 (8)	C_{29}	303 (15)	560 (37)	924 (44)
$C_{3.6}$	1508 (3)	−786 (7)	6827 (8)	C_{212}	2974 (2)	−1421 (6)	10477 (8)	C_{30}	150 (24)	993 (57)	925 (65)
$C_{4.6}$	1731 (3)	−503 (7)	7409 (8)	C_{312}	3186 (2)	−1852 (6)	10901 (8)	C_{31}	−186 (14)	1544 (32)	324 (41)
$C_{5.6}$	1817 (3)	160 (7)	7313 (8)	C_{412}	3456 (2)	−1568 (6)	11289 (8)	O_3	575 (7)	−199 (17)	2138 (22)

[a] Coordinates multiplied by 10^4, temperature factors by 10^3.

Computational Details. All of the MO calculations were of the extended Hückel type using a modified version of the Wolfsberg–Helmholz formula.[38] The parameters used for Co, O, and C atoms are taken from ref 39. The H_{ii} for hydrogen is −13.6 eV, and the Slater exponent is 1.3. The (triphos)Co fragment was simulated with a H_3Co fragment with Co–H distances of 1.7 Å and H–Co–H angles of 90°. The geometry of the quinoid ligand was kept fixed in all calculations, irrespective of the total electron population: the C–C and C–O distances were fixed at 1.4 and 1.3 Å, respectively.

Acknowledgment. Thanks are due to Dr. Stefano Midollini for providing part of the initial impulse for this work. We also thank Dr. Alessandro Bencini for stimulating and helpful discussions, particularly as related to the interpretation of the EPR spectra. This work was partially supported by a CNR grant "Progetto Bilaterale" to C.B.

Registry No. **1**, 110315-70-3; **2**, 110315-72-5; **3**, 110315-73-6; **4**, 110315-74-7; **5**, 110315-76-9; **6**, 110315-84-9; **7**, 110315-78-1; **8**, 110315-80-5; 3,5-DBQ, 3383-21-9; *o*-Cl_4Q, 2435-53-2; phenQ, 84-11-7; [(triphos)Co(μ-Cl)$_2$Co(triphos)]$(ClO_4)_2$, 110315-82-7; $Co_2(CO)_8$,

(38) Ammeter, J. H.; Bürgi, H.-B., Thibeault, J. C., Hoffmann, R. *J. Am. Chem. Soc.* **1978**, *100*, 3686.

(39) Albright, T. A.; Hoffmann, P.; Hoffmann, R. *J. Am. Chem. Soc.* **1977**, *99*, 7546.

10210-68-1; [(triphos)Co($O_2C_7H_5$)]$^{2+}$, 110315-85-0; [(triphos)Co($O_2C_7H_5$)], 110315-86-1; [(triphos)Co(3,5-DBQ)]$^{3+}$, 110315-96-3; [(triphos)Co(3,5-DBSQ)]$^{2+}$, 110315-98-5; [(triphos)Co(3,5-DBCat)], 110352-17-5; [(triphos)Co(3,5-DBCat)]$^{-}$, 110315-87-2; [(triphos)Co(*o*-Cl_4Q)]$^{3+}$, 110315-95-2; [(triphos)Co(*o*-Cl_4SQ)]$^{2+}$, 110315-97-4; [(triphos)Co(*o*-Cl_4Cat)], 110453-57-1; [(triphos)Co(*o*-Cl_4Cat)]$^{-}$, 110315-88-3; [(triphos)Co(phenQ)]$^{3+}$, 110315-99-6; [(triphos)Co(phenSQ)]$^{2+}$, 110316-00-2; [(triphos)Co(phenCat)], 110432-95-6; [(triphos)Co(phenCat)]$^{-}$, 110315-89-4; [H_3Co(Cat)]$^{3+}$, 110315-90-7; [H_3Co(Cat)]$^{2+}$, 110315-91-8; [H_3Co(Cat)]$^{+}$, 110315-92-9; [H_3Co(Cat)], 110315-93-0; [H_3Co(Cat)]$^{-}$, 110315-94-1.

Supplementary Material Available: Listings of hydrogen atom coordinates and final anisotropic and isotropic thermal parameters for **2** (6 pages); a listing of observed and calculated structure factors (30 pages). Ordering information is given on any current masthead page.